Original Article

Performance Optimization of an Archimedean Screw Turbine a Hydropower Generator for Sustainable Energy Generation

Jennery Brian Sobel¹, Joven Buhia¹, CristyMae Tino¹, John Marrie Lambot¹, Alberto E. Lastimado Jr^{1*}

¹Engineering Department, North Eastern Mindanao State University, Surigao del Sur, Philippines.

*Corresponding Author: alastimado@nemsu.edu.ph

Received: 08 August 2025 Revised: 09 September 2025 Accepted: 10 October 2025 Published: 31 October 2025

Abstract - This study presents details on how researchers developed a low-cost, portable hydro generator that utilizes an Archimedean screw design and addresses the problem of sustainable energy sources in remote locations. In the work design, variables were subject to optimization. Efficiency overall saw improvement, too. Laboratory testing was used to develop a prototype. Blade width plus inclination angle were design variables for testing using Response Surface Methodology, a Central Composite Design. Discharge, input power, output power, and efficiency were the performance response measurements taken. Performance was indeed strongly related to both design variables through linear, quadratic, and interaction relationships according to ANOVA. RSM standardized the optimum to a blade width of 34.9 mm along with an angle of inclination of 20.5°, which led to an efficiency of 72.6% with relatively low input power (3.18 W) and near maximum output power (2.39 W). The model provided an adequate fit because lack-of-fit tests did indicate no meaningful lack of fit, and the R² values were high. These results suggest portable Archimedean screw turbines could develop micro-hydropower affordably for decentralized and off-grid energy needs.

Keywords - Archimedean Screw Turbine, Efficiency optimization, Portable hydro generator, Response Surface Methodology, Sustainable energy.

1. Introduction

The persistent challenge of energy poverty greatly hinders socio-economic development, especially in remote and rural communities in which extending conventional grids is often economically and logistically unfeasible [1]. Electricity access is still lacking for more than 666 million people around the globe, especially within Sub-Saharan Africa, where the shortage overwhelmingly concentrates in the rural areas. Healthcare is constrained, educational opportunities are limited, and economic growth is stifled by this unreliable power; decentralized off-grid energy solutions are critically needed [2]. Micro-Hydropower (MHP) generates continuous, reliable power and impacts the environment minimally, especially in "run-of-river" configurations [3, 4], so it offers a compelling alternative among available renewable technologies.

Despite its potential, the common adoption of Micro-Hydropower (MHP) is often obstructed by a dependency on specialized manufacturing, high upfront capital costs, and the technical expertise required for installation and maintenance [5, 6]. Such an issue does create a critical technology-adoption gap, especially in pico-hydropower scales that are less than 5 kW and in nano-hydropower scales that are less than 100 W, which ideally suit individual households or small community clusters in remote areas with low-head water resources under 5 meters and low flow [3, 7]. The Archimedean Screw Turbine (AST) seems attractive. It is particularly compelling within these conditions. It is economical for fabrication and for operation, has a lower environmental impact overall, and is highly effective within the low-head conditions typical of rural streams and irrigation canals as a quasi-static pressure turbine [4, 5, 8].

Nevertheless, a key obstacle remains. That challenge obstructs the technology's full potential for rural electrification. For AST design, standardized analytical guidelines are often ignored, especially for portable as well as pico-scale applications, and designer experience or ad hoc methodologies are instead relied on [4, 5]. The lack of a systematic design framework significantly hinders the replication and deployment of ultra-low-cost, locally manufacturable systems. Manufacturing infrastructure is often lacking in developing regions. This exacerbates the problem, as these regions are also unable to plan or evaluate their viability [6].

Therefore, this study addresses the central research gap by highlighting the absence of a rigorously optimized and experimentally validated framework for constructing a portable AST using widely available low-cost materials. This research employs a systematic optimization methodology instead of a basic proof-of-concept to create a more adaptable compendium for developing convincing, context-applicable energy solutions. This work searches for an avenue toward democratizing design processes. Incorporation of polyvinyl chloride, or PVC, a readily available resource, aids in achieving this. Response Surface Methodology, or RSM, a method for statistical enhancement, additionally empowers local communities to construct and preserve enduring energy infrastructure.

1.1. Novelty and Contribution

The chief contribution of this research lies in its method for fashioning an effective, accessible pico-hydropower resolution that is both systematic and holistic. This revolutionary synthesis presents material science, practical design, and strict optimization methodology. Earlier investigations probed discrete aspects germane to AST design. Three linked principles represent the factors that may determine innovation.

- 1. Material Innovation: This exploration transcends the typical applications for steel. It advances material technology. It enhances our understanding of the subject through detailed examination. The turbine's existence is, as a whole, a Polyvinyl Chloride (PVC) construction. Each of the helical blades has been incorporated. This allocated resource directly addresses the cost impediment. Selecting it elucidates that point. Production intricacy is likewise challenging it. This obstructs the implementation of MHP within isolated populations [4, 5]. Fundamental implements enable those who utilize PVC to construct edifices because they diminish the skill threshold for indigenous construction and upkeep and improve technological availability [9, 10].
- 2. Innovate design so it is for portability and resilience: The design ethos stresses portability and resilient function, attributes vital to off-grid implementations. The reduced density of PVC facilitates transportation to remote locations, which presents a logistical challenge for MHP systems [4]. Furthermore, they incorporate screen filtration immediately to confront the common functional issue of detritus, which can impair and erode [11, 12].
- 3. Optimization's Methodological Innovation: In regard to an inaugural demonstration concerning a pico-scale, PVC-based AST, this analysis employs Response Surface Methodology (RSM), which is a stringent statistical method. Engineers create specific designs throughout practice [4] using RSM to improve larger, recognized turbines [13], and the application validates its factual framework. The study discerns statistically meaningful linear and quadratic interaction effects. The width of the

blade and the angle of inclination combine to produce observable effects. Therefore, a practical design blueprint that increases efficacy is available within the defined scope and resource limitations. These three constituents generate a cooperative interaction. Science certainly progresses considerably today. This exploration evinces that engineers are able to optimize accessible low-cost materials so that they may resolve energy poverty holistically and appropriately.

2. Literature Review

2.1. Pico-Hydropower for Rural Electrification

This study is classified within pico-hydropower's wideranging domain, for systems that generate power below 5 kW. "Household hydro" constitutes a designation frequently employed for pico-hydro. It is additionally acknowledged as rather economical. This type of generator is perceived as an enduring electrification option for impoverished residences. These far-flung locales are frequently without connectivity. Diesel generators or renewables such as solar PV and wind possess an elevated lifetime cost compared with pico-hydro and yield a diminished, reliable power output [3]. It harnesses the natural flux from waterways and irrigation channels lacking substantial water impoundment or wide-ranging barriers because it diminishes ecological repercussions [4, 7].

Pico-hydro implements its deep socio-economic benefits. Dependable electricity access elevates educational results through evening study illumination, betters healthcare via vaccine refrigeration and medical device power, and curtails air contamination through kerosene displacement. Regional economics may discover utility, too. Earning revenue may engender novel prospects. Examples from developing nations, such as Nigeria and Vietnam, show that portable pico-hydro generators can provide essential electricity while often emphasizing local resources, as these generators reduce costs and improve serviceability. Nevertheless, important impediments deter common acceptance because endeavors collapse frequently. Gear might exhibit inferior quality, turbines might be inappropriately designated, indigenous technical skill may be absent for upkeep, or fabrication infrastructure throughout isolated areas may be inadequate [14].

2.2. Advances in AST Design and Optimization

The performance concerning an Archimedean Screw Turbine (AST) is quite sensitive to geometric parameters; therefore, wide-ranging research optimizes its architecture while researchers employ it diversely. The cant angle constituted one important characteristic that was scrutinized. The quantity of the blades was also subjected to investigation. The screw pitch was likewise aligned. Innumerable investigations have validated that a prime tilt angle generally resides at 20° and 25°. As this spectrum counteracts the gravitational force component, effective fluid entry is allowed in the Archimedes screw channels. Reference [8] determined

that a five-blade screw optimally performed its functions at inclination angles ranging from 20° to 24.5°. Reduced inclinations rendered three-blade configurations suitable for illustration.

The number of blades also plays a critical role. Their magnitude bears great importance. [15] demonstrated empirically that just improving the quantity of blades could increase efficiency along with power generation capacity under those ultra-low head conditions. Although advancement diminished thereafter, effectiveness peaked close to seven units. Likewise, screw orientation impacts the liquid volume. This amount is procured during each cycle. Substantial tribological impairments may arise if an expanded helix, which increases torque, lacks proper adjustment.

Since these variables interact, statistical optimization approaches are effective. [13] utilized Response Surface Methodology to improve blade inclination, stride, and diameter ratios suited for hydrokinetic implementations, for example, because they demonstrated the value of these types of techniques while perfecting AST configuration. These investigations stress maximizing numerous variables since the optimal arrangement frequently exchanges detailed elements. Volumetric introduction accompanied by effluent diminutions correlates reciprocally with kinetic impedance. Deficient are the analysis instructions, which remain a key encumbrance despite these advancements. Several blueprints still depend upon the builder's history; therefore, this imperfection stresses the requirement for optimization frameworks that are organized and reproducible [5].

2.3. Materials for MHP Turbine Construction

While conventional hydropower turbines typically construct these from steel because of strength, corrosion resistance, and cavitation resistance, complex manufacturing and high cost are important barriers for small-scale, decentralized applications. This issue has spurred research into alternative materials for MHP technology access.

Polyvinyl chloride, or PVC, is employed in MHP components such as penstocks and turbine casings or blades, so that construction becomes simplified since costs become reduced as documented. Reduced expenditure, coupled with intrinsic invulnerability to corrosion, represents the merits of PVC. Its facile creation via simple implements is additionally helpful for regional production and agrarian upkeep. Specifically, studies throughout the Philippines fabricated PVC-based ASTs. They evinced that these ASTs serve irrigation canals. [9], Together with [10], it was affirmed that the material resolves low-head applications economically.

Implementations demanding greater tenacity relative to heft are being investigated. Fiber-reinforced composites are contemplated for these implementations. In this context, they are certainly an outstanding substitute. Substances like fiberglass or carbon fiber-reinforced polymers are notably lighter. These materials can contend with steel in terms of fatigue strength and stability. In view of its provision of design adaptability in conjunction with its elite corrosion resistance, this technology has become established in applications for wind turbine blades. However, composites generally entail elevated costs regarding materials and also withstand cavitation erosion to a greater degree than steel; thus, investigators must evaluate a cost-performance tradeoff regarding every separate application [9, 11]. Additive manufacturing (3D printing) has also materialized as a practical production technique for diminutive, prototype-scale turbines because it fashions detailed configurations with great exactitude [16]. The current investigation augments the manner in which PVC exists as viable via rigidly refining a completely PVC-utilized turbine since the investigation aims to perform absolutely while preserving the important benefits involving minimal expense with simple fabrication.

2.4. Micro-Hydropower Implementation in Southeast Asia

The development of this portable AST generator is directly informed by both successes and challenges in rural electrification efforts across Southeast Asia, especially in the Philippines. For the Philippine archipelago, there is an important untapped potential for MHP, estimated at 27,000 kW. This capability supports the government's aim for complete village electrification [17]. As of 2013, over 100 MHP locales possessed capabilities extending from 0.03 kW to 75 kW since they chiefly powered illumination plus minor apparatuses within isolated hamlets [17].

The principal model executes these undertakings by government or private/NGO subventions while forcefully emphasizing communities engaging with and donating, frequently via pro bono labor [17]. Prevailing factors like Parina and Timodos highlight the Philippines' MHP undertakings. Individuals underwent ownership, individuals affiliated with society, and this remained fundamental within both regions. Individuals engaged in these activities commencing with preparation through the undertaking of maintenance [17]. De La Salle University within Parina and YAMOG inside Timodos positioned themselves to champion such initiatives. A socioeconomic nucleus impacted these exhibited endeavors. Superior educational achievements were displayed by students who studied at night. Their health improved upon the decline of kerosene lamp employment. This diminished usage proved helpful. [17] incorporated novel approaches for generating revenue, such as welding services and appliance repair, into that, too. ₱600 toward monthly savings was documented by Timodos households via lessened kerosene costs [17].

The region's diverse divisions echo throughout this cooperative progression model. Notably, Indonesia's IBEKA project spurred rural development greatly through the

engagement of local communities during the MHP process. Toward ownership as well as conservation, this endeavor fosters native skill and ensures edifices fulfill local stipulations [18]. An inquiry across Bawan Valley, Borneo, likewise discovered MHP systems prosper more when communities build capacity together with stakeholders, involving themselves rather than when merely technical aspects drive their success while hydro resources abound [19].

These specific investigations bring into focus prominent quandaries in any case. Those challenges are persistent. A major problem arises when locales lack sufficient expertise for resource maintenance. This dilemma often strengthens since the locales possess geographic isolation. References [17] and [19] confirm this segregation. Considerably, the Parina case depicts how a prior pico-hydro project within the village sputtered after months because deficient turbine selection coupled with an under-capacity design stemmed from a broken turbine [17]. This accentuates an important exigency. Technologies that may prove effective are important.

Furthermore, adoption requires that these technologies possess strong accessibility. The substantiated enhancement structure immediately counters identified obstacles. The present study stresses a cheap, readily manufactured PVC design for this purpose. A technology must empower societies. Accordingly, societies are able to maintain, perform, and institute their authority decisions. Cooperative and efficient models align with this principle. They are observed throughout the region.

3. Materials and Methods

3.1. Screw Turbine Design and Specifications

The screw turbine's necessary dimensions are the outside diameter Do, inside diameter Di, angle of inclination (β), and so on. The turbine should be positioned in an inclined form [15]. Within the housing, there are helical-shaped screw blades, as a gap separates them from it. However, spinning the screw becomes easier because water leaks past it, allowing water to pass. Water travels from the upper channel over to the screw's inlet through all of the screw's blades. Water then exits at the lower end. As it goes down, water is caught between two adjacent screw blades. This process occurs from just the screw inlet to the downstream outlet. Because flowing water enters and then hits helical blades, the screw turbine turns using the water's pressure to convert to mechanical action [15]. For flowing water, Screw turbines can be installed within small, extremely low-headed storage spaces like rivers, irrigation systems, water delivery systems, drinking water systems, drainage systems, cooling systems, and even desalination plants.

Figure 1(a) shows the final appearance of the prototype through AutoCAD to ensure a 3D design feature that acts as a guide for accurate measurements, better construction, and implementation of the project. A screw turbine includes within it the housing length (L), the housing diameter (D), and the

screen filtration width (Δx). Figure 1(b) showed the required measurements for the blade's design layout. Also depicted were parameters for the blade's design structure. This includes screw length (l= 609.6 mm), inside diameter (Di = 25 mm), as well as pitch (P = 105 mm). For varying dimensions were highlighted in Figure 1(c) that had the width of blades (t = 25.4 mm, 30.2 mm, 35 mm) and inclination angles (β = 20°, 27.5°, 35°), these were based on Central Composite Experimental Design (CCD) located in Table 1. Also, this project is designed around the shaft connected to only one screw turbine blade.

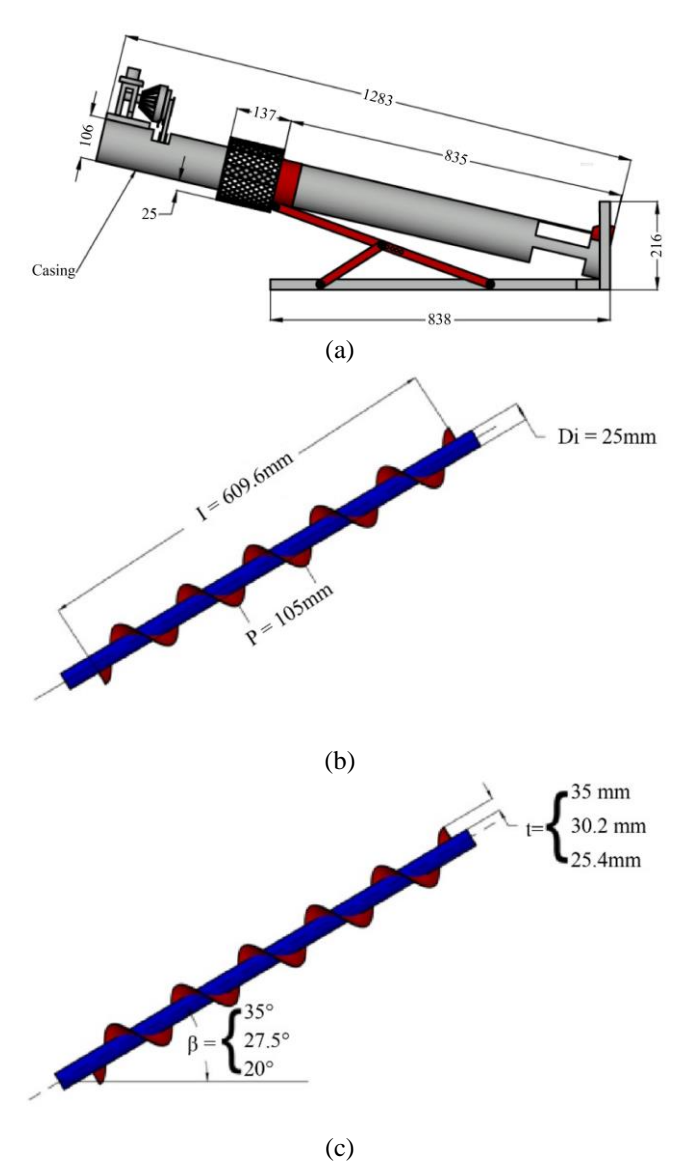


Fig. 1 (a) Screw turbine specification, (b) Screw blade dimensions, and (c) Varying dimensions of screw blade.

Heating, cutting, and bending techniques were used to design helical blades. To soften and form PVC into a spiral shape, the material is heated. The project considers a desired surface area for turbine blades that corresponds with the varying width of those blades, to produce blades that will fit the housing while having an optimal clearance between the blades and the housing. Equations 1 and 2 are used for calculating dimensions [20]. Helical blade design requires these measurements.

$$d_{bollool} = \frac{\sqrt{(d_{turbine})^2 + P}}{} \tag{1}$$

$$d_{helical} = \frac{\sqrt{(d_{turbine})^2 + P}}{\pi}$$

$$D_{helical} = D_{turbine} - d_{turbine} + d_{helical}$$
(1)

Where $d_{helical}$ and $D_{helical}$ are representative of the helical blade's inside and outside diameters (mm), respectively, $d_{turbine}$ and $D_{turbine}$ are representative dimensions of the turbine blade are inside and also outside diameters (mm), respectively, and P is defined as the screw blade's pitch (mm).

The screw received alignment following the main cylindrical housing's build. The frame was constructed to support the inclined position. Pulley assemblies exist at the top as bearings get attached at both ends, and they support the rotational motion of the shaft that can produce electricity for the generator. Lastly, the prototype is adjusted, its alignment is checked, the surface is finished, and painting is included to improve its longevity and durability.

3.2. Data Gathering

The power of the generator, known as the power output, is tested through a multimeter device that measures the values of voltage (V) along with current (I) of the generator. The turbine discharge is determined through manual calculation. The major factors that affect the design's performance, along with its waterpower (Pin).

The power from the generator (Pout) and the overall efficiency (e) are factors too. Equations 3-5 were used to calculate the discharge, the effective head, and the power input. Equations 6 and 7 were used for the calculation of the power output and overall efficiency.

$$Q = \frac{Volume}{Timeelapsed} \tag{3}$$

$$H = lsin \beta \tag{4}$$

$$P_{in} = Q\gamma H \tag{5}$$

$$P_{out} = Voltage \times Current$$
 (6)

$$e_o = \frac{P_{out}}{P_{in}} \times 100\% \tag{7}$$

Where Q represents the discharge $(\frac{m^3}{s})$, L as screw length (m), β as inclination angle (°), P_{in} and P_{out} as input and output power (W).

The project was tested near PICOP falls in Surigao del Sur, Philippines, to evaluate performance data systematically recorded under actual conditions. We incline the turbine to ensure water flows. It is then able to operate normally. The purpose of this action is to ensure that the prototype generates power through the flowing water. Visual inspection shows that lighting up suggests the design makes power when a light bulb tests a prototype's capability.

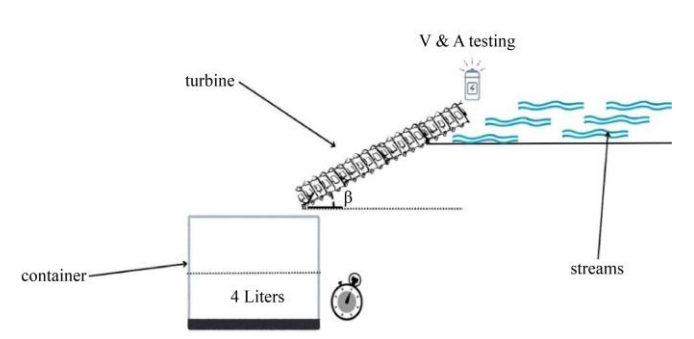


Fig. 2 Schematic diagram for the experiment setup of the Archimedean screw turbine

Figure 2 shows the arrangements that include important components for testing, such as water flow, inclined position, container, and multimeter. The schematic diagram acts as a visual guide to ensure the assembly is appropriate, as well as supporting the data gathering for testing procedures.

To ensure the reproducibility of the performance data, experimental controls were implemented for assurance of it. For each measurement set, the prototype was put in a fixed spot inside the river outflow's channeled part so the inlet flow speed stayed fairly steady. As defined by the CCD, the inclination angle (β) was precisely set and verified using a digital inclinometer for each run. The procedure that was used for measuring the discharge (Q) was standardized. In order to begin the filling process, the 4-liter container was fully submerged, and then the stopwatch was started and stopped when some water reached that volume. Even though this manual method carries a higher potential error, it is practical for field conditions as compared with a flowmeter. The turbine's rotational speed needed to stabilize prior to the time when all electrical measurements were recorded. This was in order to ensure steady-state conditions, typically after 60 seconds of continuous operation. Each of the 15 experimental runs specified in the CCD was repeated three times, and for the final analysis to minimize random errors, the average values for power input, power output, and efficiency were used.

3.3. Data Analysis

This study conducts research into Response Surface Methodology (RSM) via evaluating relationships between input variables coupled with output response and assessing the parameters [21]. A total of about 15 runs were done in the experiments. Thus, the experiments are concluded. For the

Archimedean screw turbine's performance, blade width and inclination angle are two necessary variables chosen here. In order to evaluate the behavior in relation to the variables, they selected the output responses such as discharge, voltage, current, power output, power input, and efficiency.

The maximum and minimum values should be determined in terms of the parameters the user has chosen. For the inclination angle, the maximum and minimum values are 35° and 20°, respectively. The maximum and minimum values relating to the width of blades are 35 mm plus 25.4 mm, respectively. Experiments were done in three conditions per parameter, such as maximum average, and minimum, according to Central Composite Experimental Design (CCD) [22]. One-way ANOVA lets researchers measure statistically significant variance among variables. It can also help them to observe the response. For each response model, P-values, coefficients of determination (R2), and lack-of-fit configurations were analyzed. Observed effects that unlikely chance causes are an important criterion, with a p-value less than 0.05. Authentication of model statistical importance validated the F-value calculated assessment of R2. The model's fortitude was corroborated via a lack-of-fit examination. The test differentiated between residual and pure errors. This pertained to the inaccuracies at replicated locations.

4. Results and Discussion

Table 1 shows exactly what the experimentation that RSM hinged upon engendered. For the determination of the performance stemming from each run, they judged this project to conform to experimental factors such as blade width as well as inclination angle. Furthermore, the Design Expert software's RSM method data will be illuminating. The evidence shall show the outcomes. Comprehension of consequences is augmented via these details. The experimentation's documented values are predicated upon all the responses.

4.1. Analysis of Variance on Power Input, Power Output, and Efficiency

The Analysis Of Variance or ANOVA for the response variables, which include power input, power output, and efficiency, showed reliable explanations for the observed variations plus statistical significance regarding the fitted models.

Power input shown in Table 2 revealed that such a cubic model was indeed highly important since F=754.63 when p was less than 0.0001, which indicated superb model adequacy. The response was found to be strongly influenced by main effects inclination ($F=271.23,\ p<0.0001$) along with the width of blades ($F=372.19,\ p<0.0001$). Furthermore, interaction and quadratic terms were indeed meaningful. This importance, interaction via AB, $F=541.79,\ p<0.0001$ and quadratic terms via $A^2,\ F=499.89,\ p<0.0001;\ B^2,\ F=85.22,\ p<0.0001;\ A^2B,\ F=156.66,\ p<0.0001,\ indicated nonlinear$

and synergistic effects. That confirmed the model adequately represents the data, so the lack-of-fit test was not important (p = 0.0576). An Adeq Precision of 107.35 was high and supported the very strong statistical fit since $R^2 = 0.9987$, Adjusted $R^2 = 0.9974$, Predicted $R^2 = 0.9286$. In Table 3, coefficient estimates show that blade width negatively influenced power input (-3.87). Inclination exerted a positive effect on the course (+3.30). The curvature and combined influences of the factors were stressed further by strong quadratic and interaction contributions. The findings suggest that the system's power input requirement is substantially determined by higher-order and linear terms.

Power output at Table 4, the quadratic model was furthermore meaningful (F = 118.54, p < 0.0001), as highlighted. Prevailing components materialized inclination (F = 93.78, p < 0.0001) along with blade width (F = 393.14, p < 0.0001). Nevertheless, their interplay lacked importance. The statistical value equaled AB, p = 0.6631. The presence of largely autonomous effects is indicated via this outcome. Blade width evinced a marked quadratic influence given its relation to curvature (A², F = 70.91, p < 0.0001) that researchers noticed, though inclination squared (B2, p = 0.1601) proved inconsequential. The discordance was critically divergent (p < 0.0001) from the power input. It also evinced that, although the model seized much of the variability, unexplained deviations still remain. Model suitability existed given $R^2 = 0.9850$, Adjusted $R^2 = 0.9767$, and Predicted $R^2 = 0.8515$. Adeq Precision augmented its endorsement. That support totalled 38.10. Coefficient estimates affirmed positive contributions stemming from inclination (+0.1369) and blade width (+0.2804) based on Table 5. Specifically, quadratic effects, including A² (-0.1716), displayed diminishing returns beyond elevated blade widths. The suggestion is that blade width impacts power output critically; however, efficiency diminishes beyond its most desirable point. Exhibiting an outstanding statistical importance measure (F = 198.30, p < 0.0001), the quadratic model in Table 6 furnished the optimal suitability for efficacy. Large impacts were manifested via blade width (F = 403.24, p < 0.0001) along with inclination (F = 469.58, p < 0.0001). Their interplay was additionally important (AB, F = 39.03, p = 0.0002) with resultant response impacted via conjoint variable gradations. Blade width squared evinced an important quadratic impact (A², F = 74.81, p < 0.0001). Predilection squared nevertheless lacked an important quadratic consequence (B^2 , p = 0.0939). The lack-of-fit test was inconsequential because p = 0.2353. This outcome additionally validates the model's dependability. Statistical measures again confirmed robustness because $R^2 = 0.9910$, Adjusted $R^2 = 0.9860$, Predicted $R^2 = 0.9543$, and Adeq Precision = 53.90. Coefficients revealed that blade width strongly affected efficiency positively (+16.28) while inclination impacted it negatively (-17.57). The interaction term (-6.20) and quadratic term ($A^2 = -10.11$) in Table 7 show that extreme factor adjustments may harm efficiency. To prevent energy losses from overextended design parameters, these results suggest balancing blade width with inclination to maximize efficiency.

Overall, the ANOVA and RSM findings across all three responses indicate that blade width with inclination influence parameters highly, contributing in a linear way and nonlinearly strongly. The models' exceptionally high R^2

values as well as favourable Adeq Precision statistics confirm that they are reliable for predictions. Curvature and interaction terms are quite meaningful, however. Optimal performance needs more than linear adjustments; therefore. Careful optimization of both parameters is required instead to maximize power output and efficiency while minimizing power input.

Table 1. Recorded values of the experiment

Run	A: Width of Blades	B: Inclination	Power input	Power output	Efficiency
	(mm)	(0)	(W)	(W)	(%)
1	30.2	27.5	5.36182	2.4258	45.2421
2	35	35	9.33357	2.6715	28.6225
3	30.2	27.5	5.75279	2.4232	42.1222
4	30.2	27.5	5.8441	2.4219	41.4418
5	25.4	20	6.06027	1.7563	28.9806
6	25.4	35	25.4081	2.0982	8.25801
7	25.4	27.5	12.9945	1.9929	15.3365
8	30.2	20	3.63616	2.301	63.281
9	35	27.5	5.25969	2.4973	47.48
10	30.2	27.5	5.8441	2.4219	41.4418
11	30.2	27.5	5.36182	2.4258	45.2421
12	30.2	27.5	5.75279	2.4232	42.1222
13	35	20	3.18341	2.3608	74.1595
14	30.2	35	10.2391	2.47	24.1233
15	30.2	27.5	5.8441	2.4219	41.4418

Table 2. Analysis of variance on power input

Source	Sum of Squares	Df	Mean Square	F-value	p-value	
Model	424.56	7	60.65	754.63	< 0.0001	Significant
A-Width of Blades	29.91	1	29.91	372.19	< 0.0001	
B-Inclination	21.80	1	21.80	271.23	< 0.0001	
AB	43.54	1	43.54	541.79	< 0.0001	
A ²	40.18	1	40.18	499.89	< 0.0001	
B ²	6.85	1	6.85	85.22	< 0.0001	
A ² B	12.59	1	12.59	156.66	< 0.0001	
AB ²	1.01	1	1.01	12.57	0.0094	
A ³	0.0000	0				
B ³	0.0000	0				
Residual	0.5626	7	0.0804			
Lack of Fit	0.2687	1	0.2687	5.49	0.0576	not significant
Pure Error	0.2939	6	0.0490			Significant
Cor Total	425.12	14				
Std. Dev.	0.2835		R ²	0.9987		
Mean	7.73		Adjusted R ²	0.9974		
C.V. %	3.67		Predicted R ²	0.9286		
_			Adeq Precision	107.3454		

Table 3. Coefficients in terms of coded factors for power input

Factor	Coefficient Estimate	Df	Standard Error	95% CI	95% CI High	VIF
				Low		
Intercept	5.62	1	0.1015	5.38	5.86	
A-Width of Blades	-3.87	1	0.2005	-4.34	-3.39	3.00
B-Inclination	3.30	1	0.2005	2.83	3.78	3.00
AB	-3.30	1	0.1417	-3.63	-2.96	1.0000
A ²	3.73	1	0.1668	3.33	4.12	1.25
B ²	1.54	1	0.1668	1.15	1.93	1.25
A ² B	3.07	1	0.2455	2.49	3.65	3.00
AB ²	-0.8704	1	0.2455	-1.45	-0.2899	3.00

Table 4. Analysis of variance on power output

Source	Sum of Squares	Df	Mean Square	F-value	p-value	
Model	0.7110	5	0.1422	118.54	< 0.0001	significant
A-Width of Blades	0.4716	1	0.4716	393.14	< 0.0001	
B-Inclination	0.1125	1	0.1125	93.78	< 0.0001	
AB	0.0002	1	0.0002	0.2029	0.6631	
A ²	0.0851	1	0.0851	70.91	< 0.0001	
B ²	0.0028	1	0.0028	2.34	0.1601	
Residual	0.0108	9	0.0012			
Lack of Fit	0.0108	3	0.0036	5.86	0.065	not significant
Pure Error	0.0000	6	3.058E-06			
Cor Total	0.7218	14				
Std. Dev.	0.0346		\mathbb{R}^2	0.9850		
Mean	2.34		Adjusted R ²	0.9767	-	
C.V. %	1.48		Predicted R ²	0.8515	-	
Std. Dev.			Adeq Precision	38.0997		

Table 5. Coefficients in terms of coded factors for power output

Table 3. Coefficients in terms of coucu factors for power output							
Factor	Coefficient	df	Standard 95% CI Lov		95% CI High	VIF	
	Estimate		Error				
Intercept	2.42	1	0.0124	2.39	2.45		
A-Width of Blades	0.2804	1	0.0141	0.2484	0.3124	1.0000	
B-Inclination	0.1369	1	0.0141	0.1049	0.1689	1.0000	
AB	-0.0078	1	0.0173	-0.0470	0.0314	1.0000	
A ²	-0.1716	1	0.0204	-0.2177	-0.1255	1.25	
B ²	-0.0312	1	0.0204	-0.0773	0.0149	1.25	

Table 6. Analysis of variance on efficiency

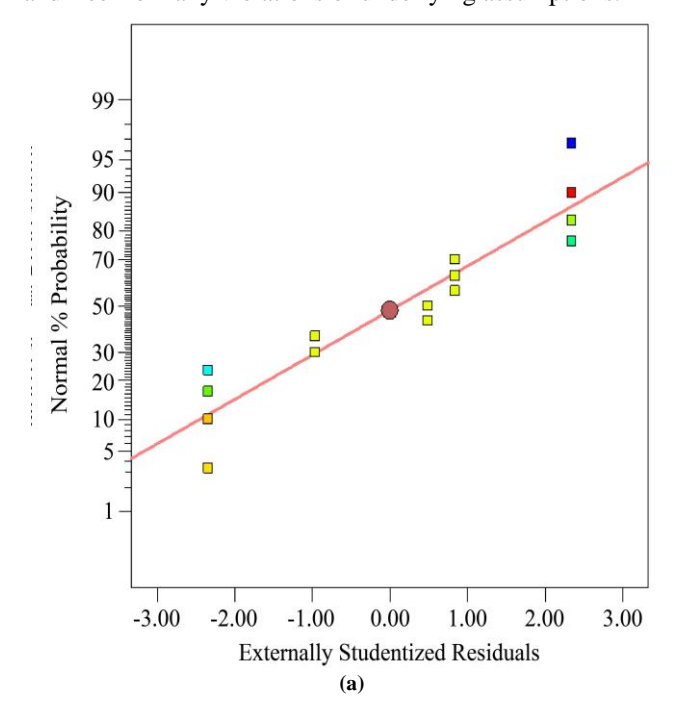
Table 6. Analysis of variance on efficiency							
Source	Sum of Squares	df	Mean Square	F-value	p-value		
Model	3910.68	5	782.14	198.30	< 0.0001	significant	
A-Width of Blades	1590.46	1	1590.46	403.24	< 0.0001		
B-Inclination	1852.13	1	1852.13	469.58	< 0.0001		
AB	153.94	1	153.94	39.03	0.0002		
A ²	295.05	1	295.05	74.81	< 0.0001		
B ²	13.83	1	13.83	3.51	0.0939		
Residual	35.50	9	3.94				
Lack of Fit	17.16	3	5.72	1.87	0.2353	not significant	
Pure Error	18.34	6	3.06				
Cor Total	3946.18	14					
Std. Dev.	1.99		\mathbb{R}^2	0.9910			
Mean	39.29		Adjusted R ²	0.9860			
C.V. %	5.06		Predicted R ²	0.9543			
			Adeq Precision	53.8999			

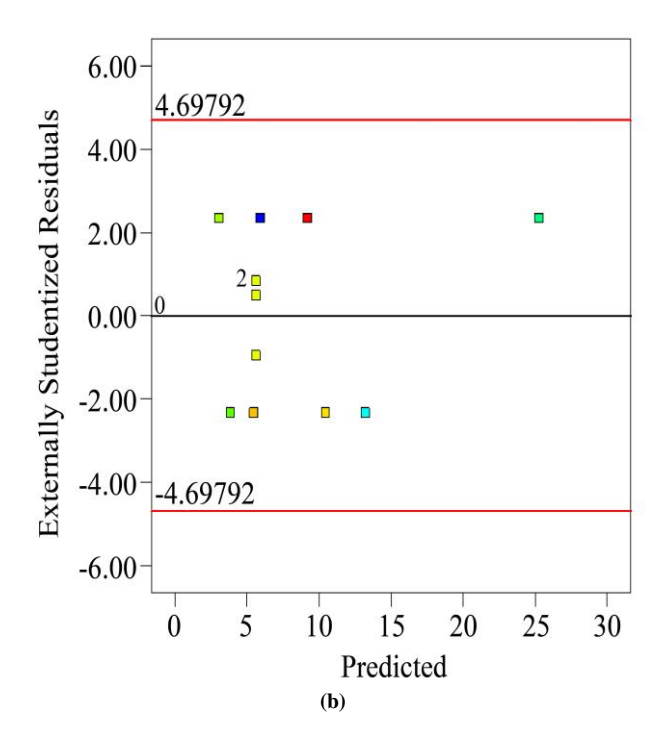
Table 7. Coefficients in terms of coded factors for efficiency

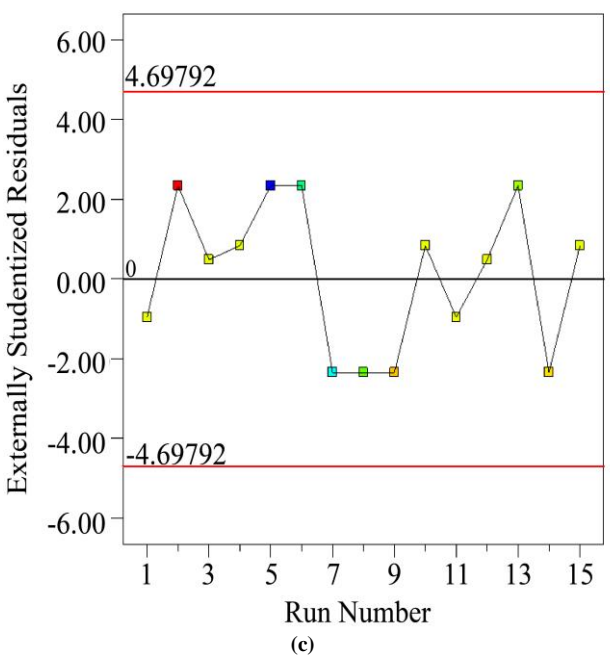
Factor	Coefficient	df	Standard Error	95% CI Low	95% CI High	VIF
	Estimate					
Intercept	42.45	1	0.7111	40.84	44.06	
A-Width of Blades	16.28	1	0.8108	14.45	18.12	1.0000
B-Inclination	-17.57	1	0.8108	-19.40	-15.74	1.0000
AB	-6.20	1	0.9930	-8.45	-3.96	1.0000
A ²	-10.11	1	1.17	-12.75	-7.46	1.25
B ²	2.19	1	1.17	-0.4553	4.83	1.25

4.2. Diagnostics for Power Input, Power Output, and Efficiency

To evaluate the validity and robustness of the ANOVA results, power input, power output, and efficiency were separately subjected to a series of diagnostic tests. For each set of figures examined, the four primary ANOVA assumptions were normality, homoscedasticity, independence, and an absence of influential outliers. Figure 3(a) presented a normal probability plot, which showed the externally studentized residuals for power input and showed that the residuals were closely aligned with the reference line. This alignment confirmed that the normality assumption was in effect. The homoscedasticity assumption was validated via the plot of predicted versus residuals in Figure 3(b), showing a random scatter around zero with no systematic pattern. Figure 3(c) depicts the run order versus residuals plot, which showed no clustering or trend. That affirmed the residuals' independence across experiment runs. Finally, the actual versus predicted plot of Figure 3(d) demonstrated that the data points aligned well along that 45-degree line, which did show strong agreement between observed and predicted. These results confirm that the ANOVA model for power input was reliable and free from any violations of underlying assumptions.







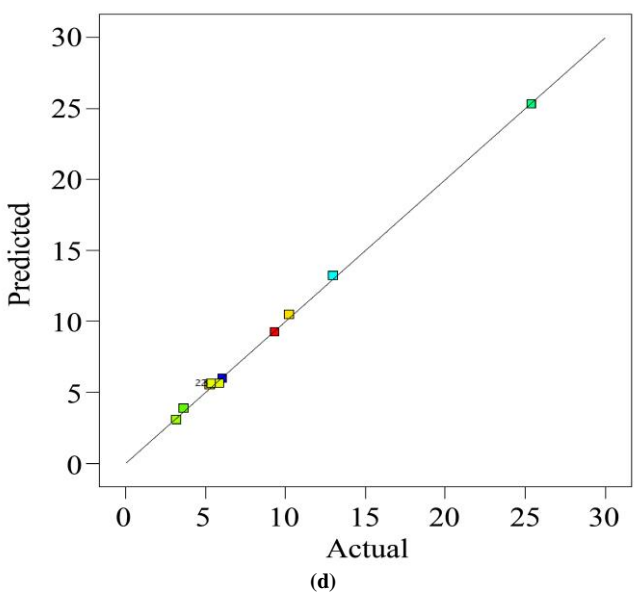
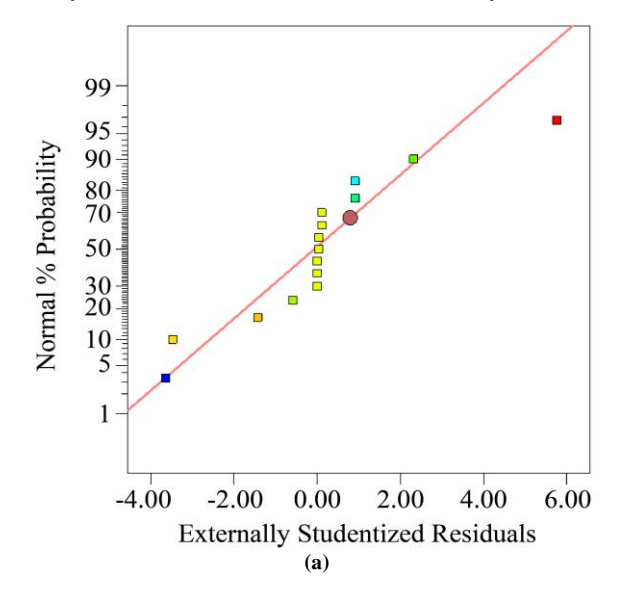


Fig. 3 (a) Diagnostics for power input of externally studentized residuals vs. Normal probability, (b) Predicted vs. Externally studentized residuals, (c) Number of runs vs. Externally studentized residuals, and (d) Actual vs. Predicted.

Power output, the normal probability plot shown in Figure 4(a), showed residuals that followed along the reference line since it indicated approximate normality. Figure 4(b) predicted versus residuals plot showed support for the assumption of homoscedasticity since residuals scattered randomly, showing no unequal variance signs. Figure 4(c) showed the run order versus residuals plot, which showed no observable sequence effects, indicating residuals were independent. Furthermore, the actual versus predicted plot within Figure 4(d) confirmed that the observed values closely agreed with the predicted ones, without detecting meaningful outliers. As these findings verify, the key assumptions toward the ANOVA model for power output were satisfied. The accuracy of its statistical inferences was thereby ensured.



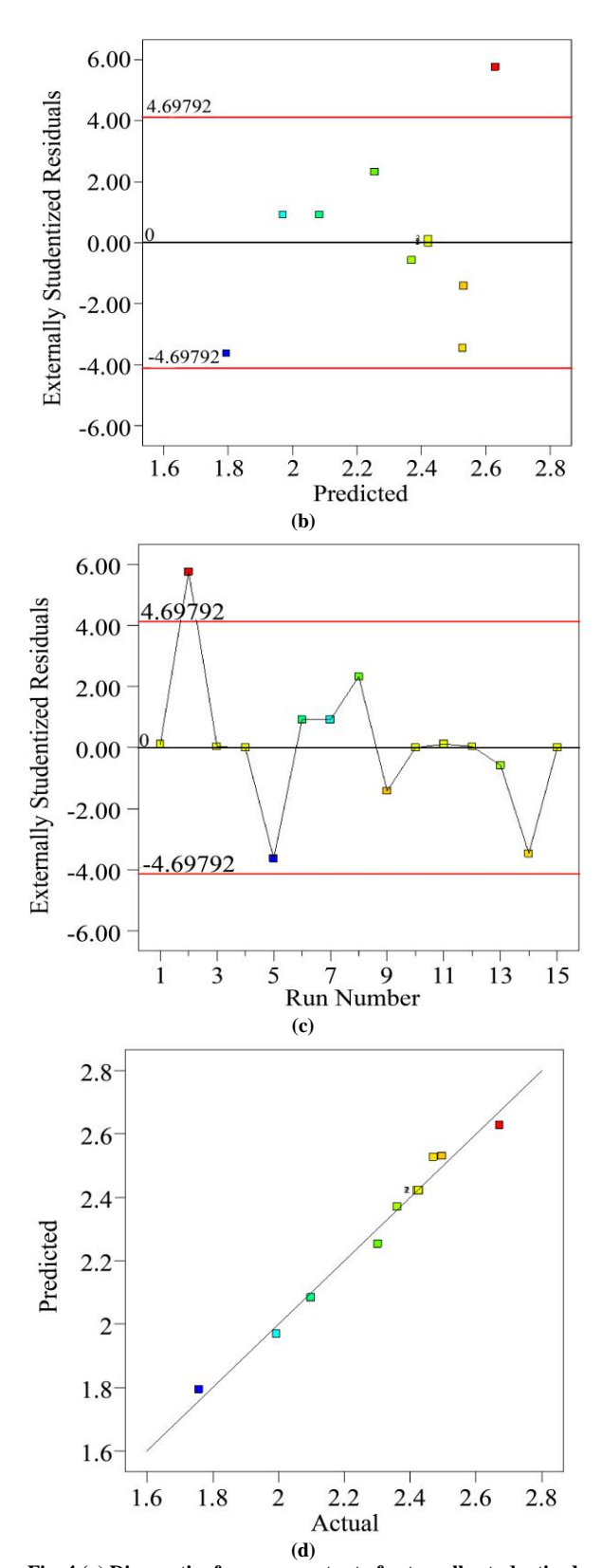
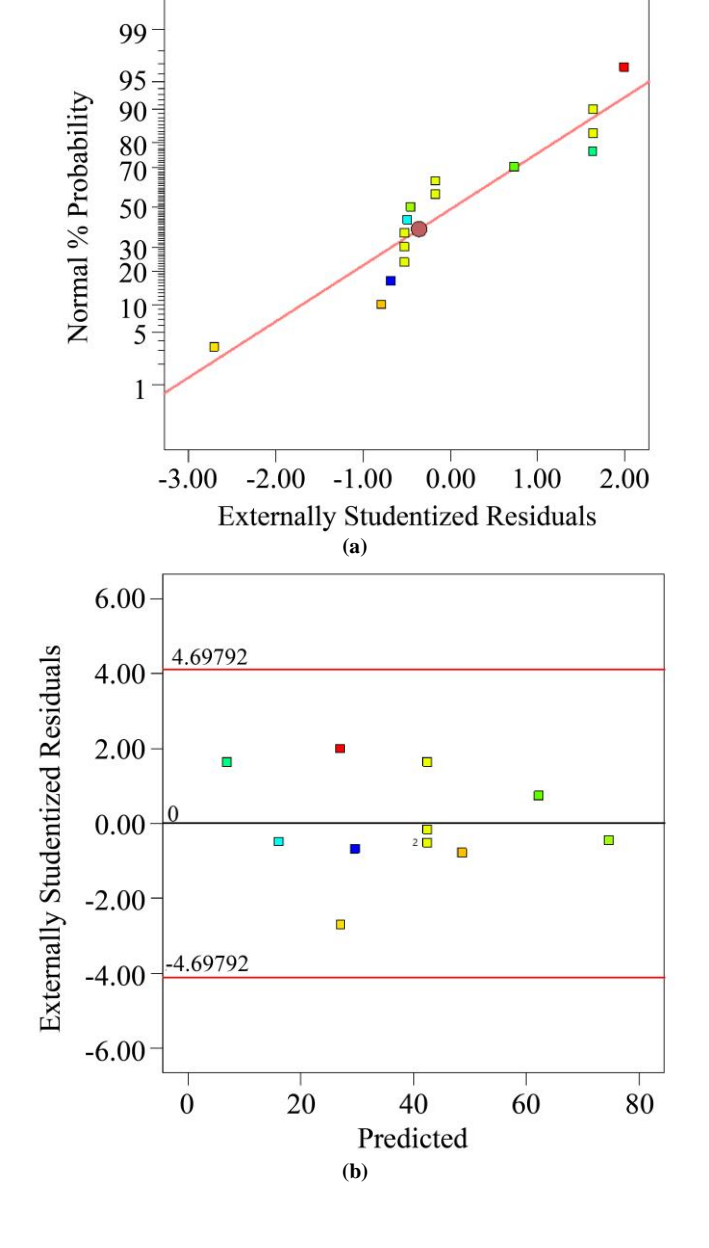
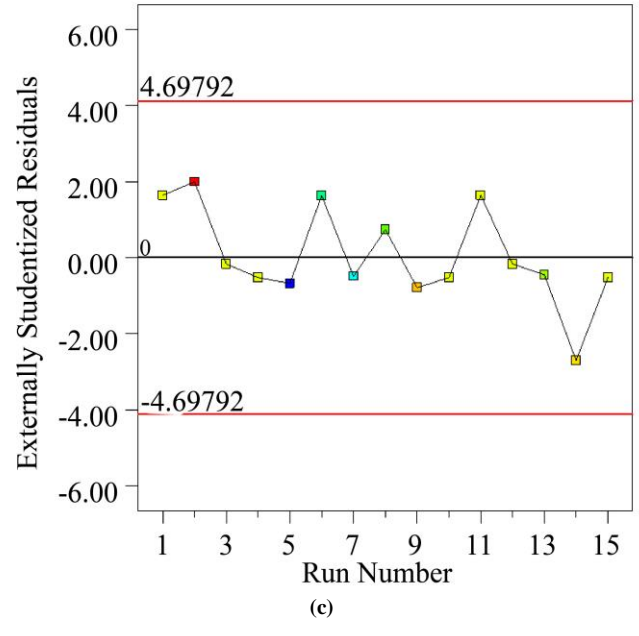


Fig. 4 (a) Diagnostics for power output of externally studentized residuals vs. Normal probability, (b) Predicted vs. Externally studentized residuals, (c) Number of runs vs. Externally studentized residuals, and (d) Actual vs. Predicted.

The normal probability plot for efficiency presented in Figure 5(a) showed nearly linear residuals, which suggested that the normality assumption was met. Homoscedasticity was validated since Figure 5(b) predicted versus residuals plot displayed a random scatter of residuals without funneling or systematic pattern. The run order in comparison with the residuals plot in Figure 5(c) showed that there was no systematic trend, and this confirmed independence for experimental runs. The trend of the plot confirmed that the runs were independent. Lastly, the actual versus predicted plot of Figure 5(d) showed a strong alignment of data points along the reference line because it reflected an adequate model fit with no influential outliers. The ANOVA results for efficiency were also strongly valid, as this indicates.





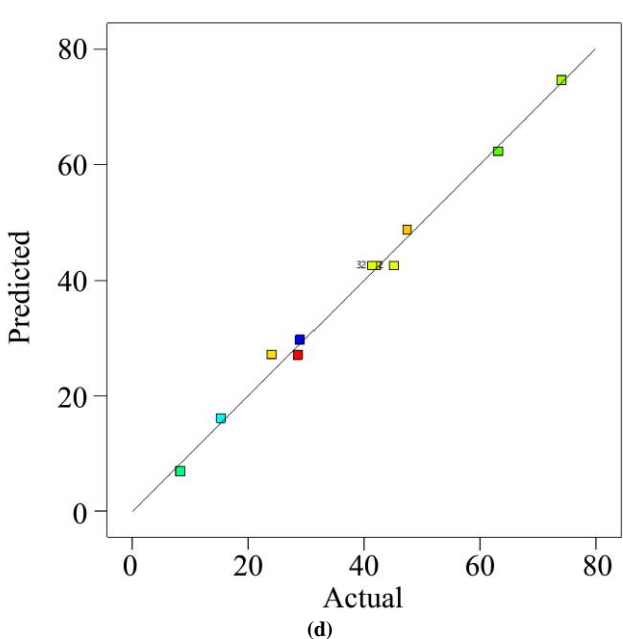


Fig. 5 (a) Diagnostics for efficiency for externally studentized residuals vs. Normal probability, (b) Predicted vs. Externally studentized residuals, (c) Number of runs vs. Externally studentized residuals, and (d) Actual vs. Predicted.

Across all three response variables of power input, power output, and efficiency, the ANOVA assumptions were met quite satisfactorily, and the diagnostic tests were confirmed. The residuals were distributed normally, the variance was homogeneous, the residuals acted independently, and we detected no influential outliers at all. Consequently, the ANOVA results can be seen as valid and reliable, so this offers a lot of support. Factors under investigation showed statistical importance.

4.3. Model Graphs for Power Input, Power Output, and Efficiency

The response surface methodology (RSM) generated three-dimensional surface and contour plots for depiction of the combined effects on the system's performance responses of the important factors (A and B), namely power input, power output, and efficiency (Figure 6).

Evaluating the fitted model's adequacy, coupled with determining the system's optimal operating conditions, requires these graphical representations by necessity.

Figure 6(a) shows the 3D surface and contour plots with power input increasing at a progressive rate. Factors A and B both rise in response. The surface presents a smooth as well as monotonic rise upwards.

We observed the very highest power input at the extreme upper levels for both variables. The energy operation requirement of the system is influenced by both factors in a strong and additive way.

Having a power of 25.4081W at a width of 25.4 mm of blades and an inclination angle of 35°, the peak values were specifically observed. To reduce operational costs, minimizing power input is desirable, but it does not necessarily align with maximum performance, so input values must be considered together with efficiency and output trends.

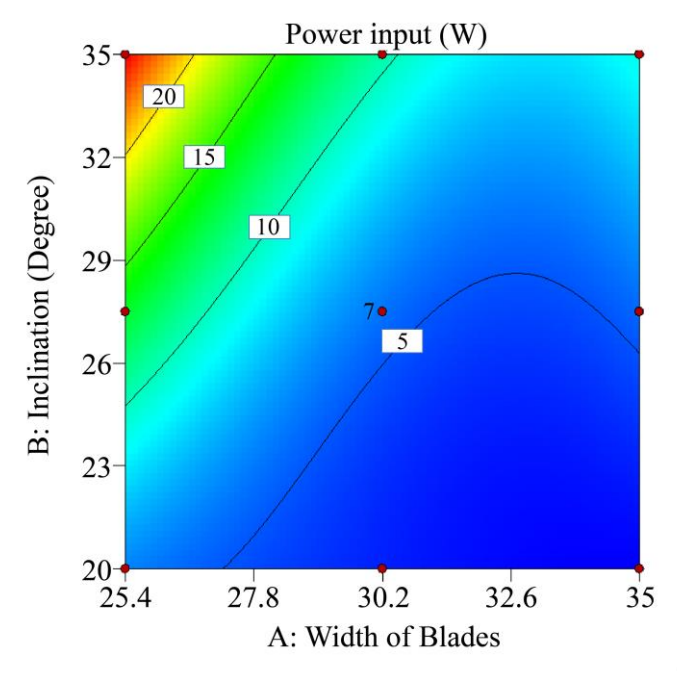
Response surface shows a nonlinear relationship for power output (Figure 6(b)) because power output peaks distinctly in a region when factor A combines with factor B at intermediate moderate-to-high levels. The elliptical patterns that are in the contour plot do suggest that the two variables interact.

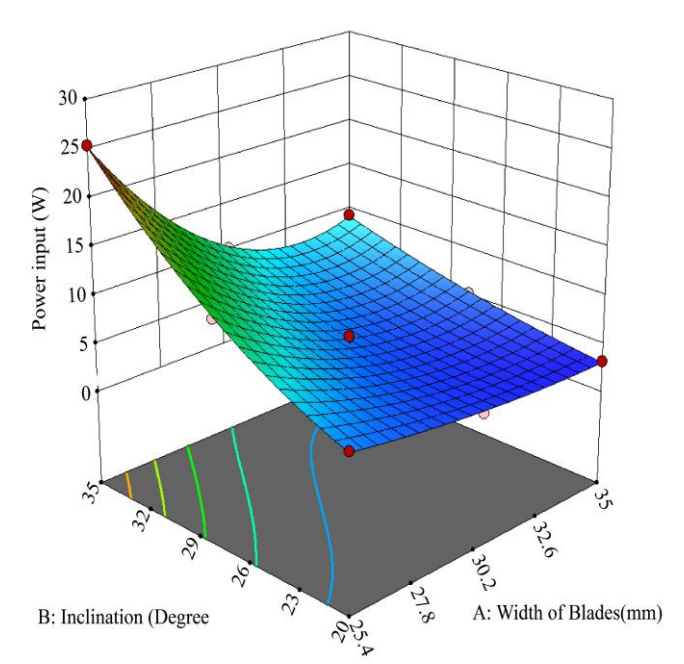
The maximum power output, which has 2.6715 W, occurs near a 35 mm blade and 35° inclination angle. Beyond the optimum region, should either factor increase further, output declines, which also indicates diminishing returns. This finding highlights that the maximum power output is just not attained at those extreme settings. Instead, it is attained from within a defined range, where factors act with synergy.

For efficiency at Figure 6(c), it was stressed that the efficiency plots incorporate the input and output effects because they execute appraisals on the system under varied conditions. Isotropic outline configurations manifest a distinct apex at moderate quantities of A and B. Efficacy is diminished greatly through excessive quantities of variables.

Indeed, the substantiation that element equilibrium is paramount persists. The maximal extent of efficiency gets to approximately 74. For a performance of 1595%, a blade width of 35 mm was employed.

Furthermore, an inclination angle of 35° was employed. Peak efficiency corresponds to the region wherein power input is moderate, with power output sufficiently high. Strong power transmutes markedly yonder.





(a)

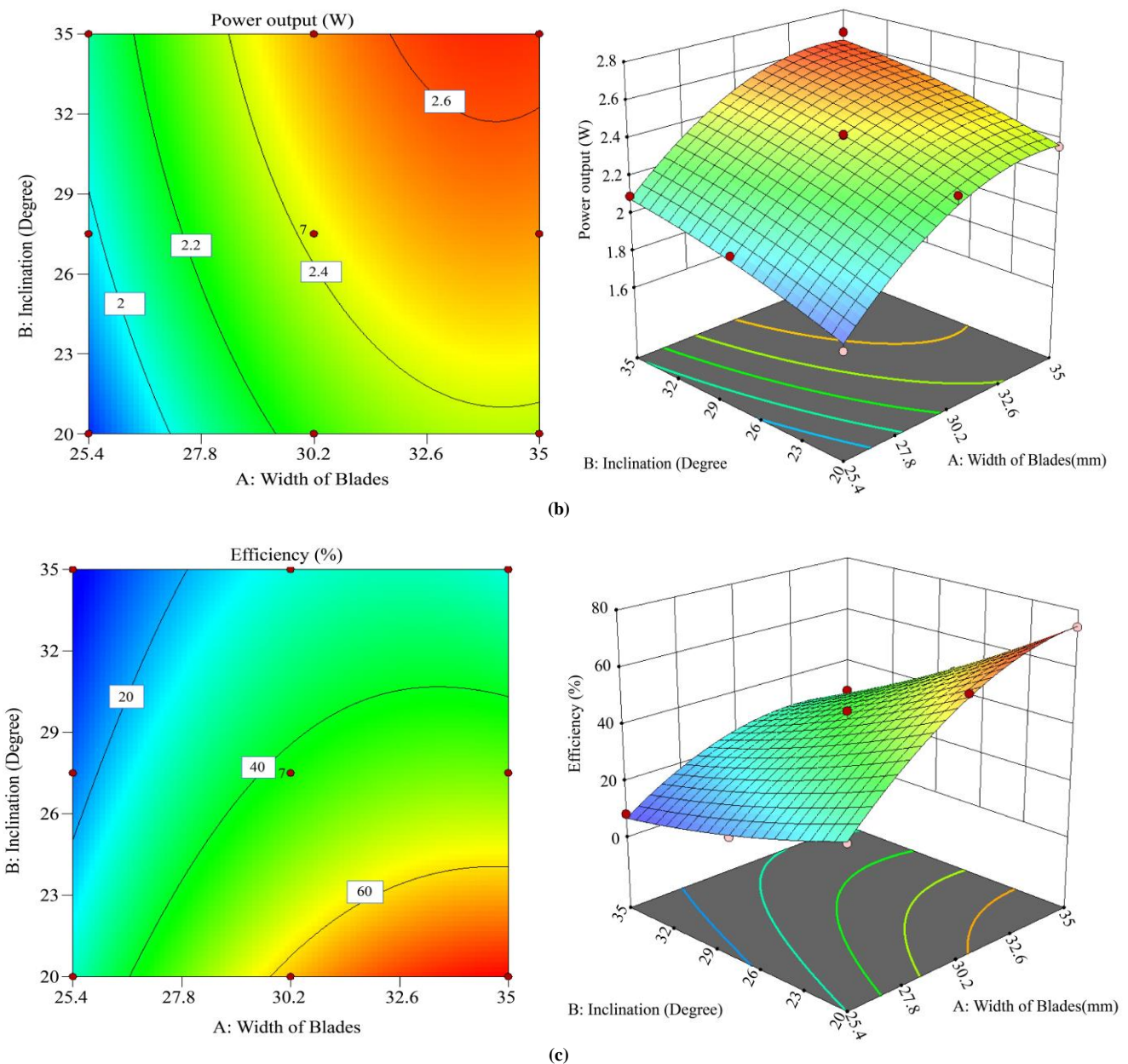


Fig. 6 Surface and Contour plots based on significant factors A and B, (a) Power input in W, (b) Power output in W, and (c) efficiency in %.

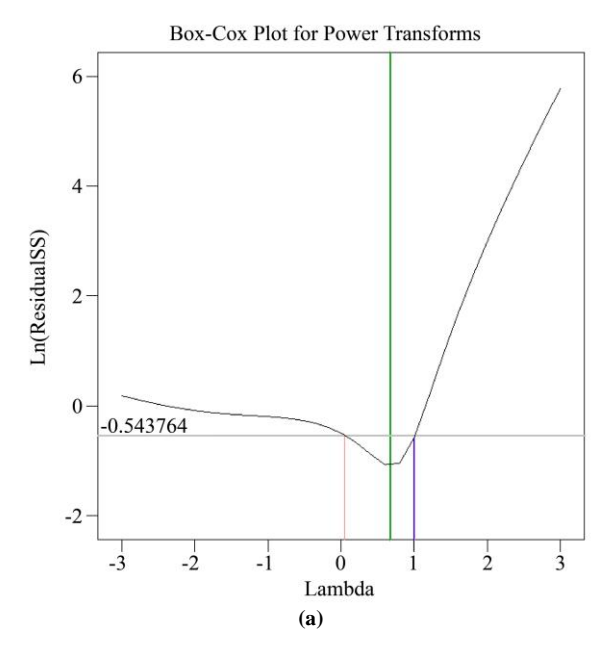
The combined interpretation of the plots indicates that power input steadily increases with factor levels. Power output peaks at moderate-to-high settings, then declines past the optimum; additionally, efficiency maximizes at intermediate levels of both A and B, where output performance plus input demand balance most favorably. These exceedingly erratic manipulations do not attain optimal operational parameters for the system.

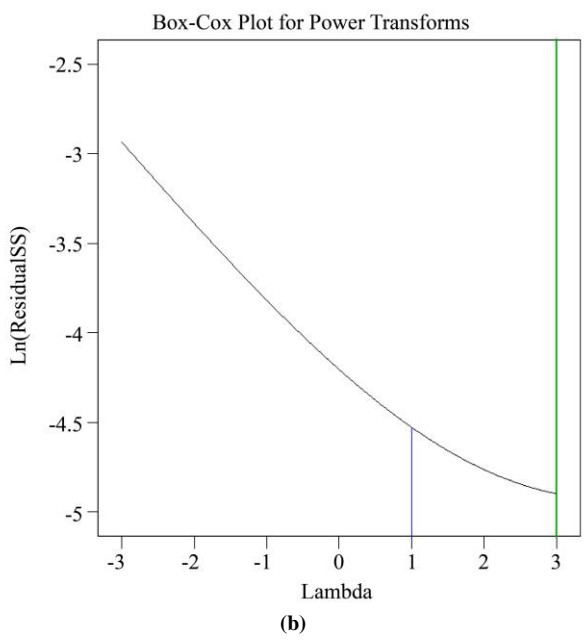
Alternatively, the variables should sustain balanced spectra to realize them. These discoveries are salient practically since they steer someone toward establishing variable plateaus. An individual may secure elevated output when they expend minimal superfluous energy.

To further validate the model, diagnostic graphs alongside model graphs were produced for visual interpretation of the relations between design variables and system performance. In order to visualize synergistic effects, there are interaction plots, including Box-Cox plots, for the assessment of data transformation, and perturbation plots, for the comparison.

In order to stabilize variance and improve the normality of the residuals, the Box-Cox plot (Figure 7) is an important diagnostic tool that is used to determine if a power transformation on the response data is necessary. Near zero is the optimal λ value shown by the peak of the curve in the Box-Cox plot for power input (Figure 7(a)). Lambda's 95% confidence interval lacks λ =1 as a value. This suggests that

transforming the power could also provide benefits. Something is indicated near the optimal value, which is near zero. Then, a logarithmic transformation can fit the power input model better. Figure 7(b)'s power output response plot shows something again. Optimal lambda is indicated to be other than 1. The curve's peak suggests someone should transform the model in order to satisfy its assumptions. The optimal lambda value happens to be very close to 1, as shown in the Box-Cox plot for efficiency (Figure 7(c)). Also, the 95% confidence interval certainly contains the value of 1. This indicates that nobody needs to transform the power for the efficiency data, so that we can reliably analyze the model using the original, untransformed response values.





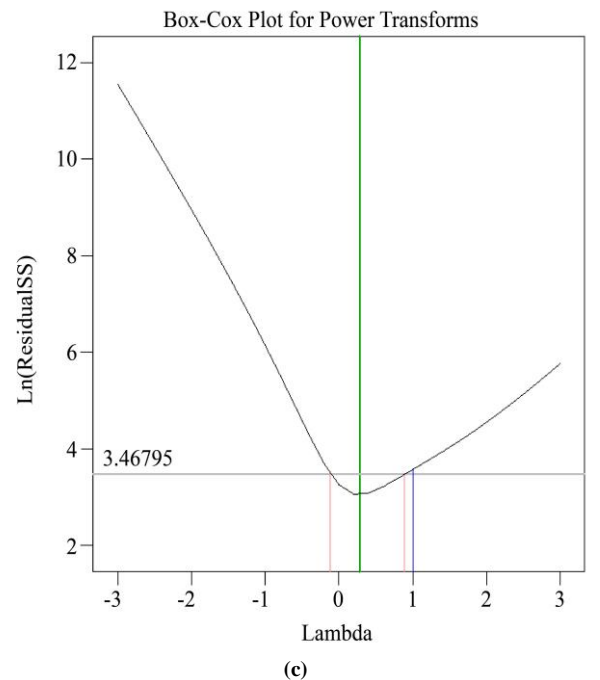


Fig. 7 Box-Cox plot for power transform, (a) Power input, (b) Power output, and (c) Efficiency.

The perturbation plot (Figure 8) helps to visualize the impact on a specific response that each design variable has at the design space's center point. A factor's line steepness indicates sensitivity.

It is the power input perturbation plot (Figure 8(a)) that reveals the important effect of the factors A (Width of Blades) and B (Inclination). The steep curves for A and B indicate a high degree of sensitivity.

The power input is highly sensitive to changes in either variable. Curvature also suggests the relationship is nonlinear instead. Factor An or Width of Blades displays a much steeper slope within the plot for power output within Figure 8(b). Factor B (Inclination) has a slope that is not of a steep nature. Visual confirmation shows that blade width has the most impact on power output.

The curve in terms of factor A also shows important curvature, which thus indicates a strong quadratic effect when power output increases along with blade width up to some optimal point prior to leveling off or declining. The efficiency perturbation plot (Figure 8(c)) shows that both factors have a deep impact.

An increase in blade width dramatically increases efficiency for the blade, and an increase in inclination angle dramatically decreases efficiency, as the steep slopes show. The pronounced curvature reinforces the ANOVA finding that a quadratic model is necessary in order to accurately capture the system's efficiency. Factor A shows this point well.

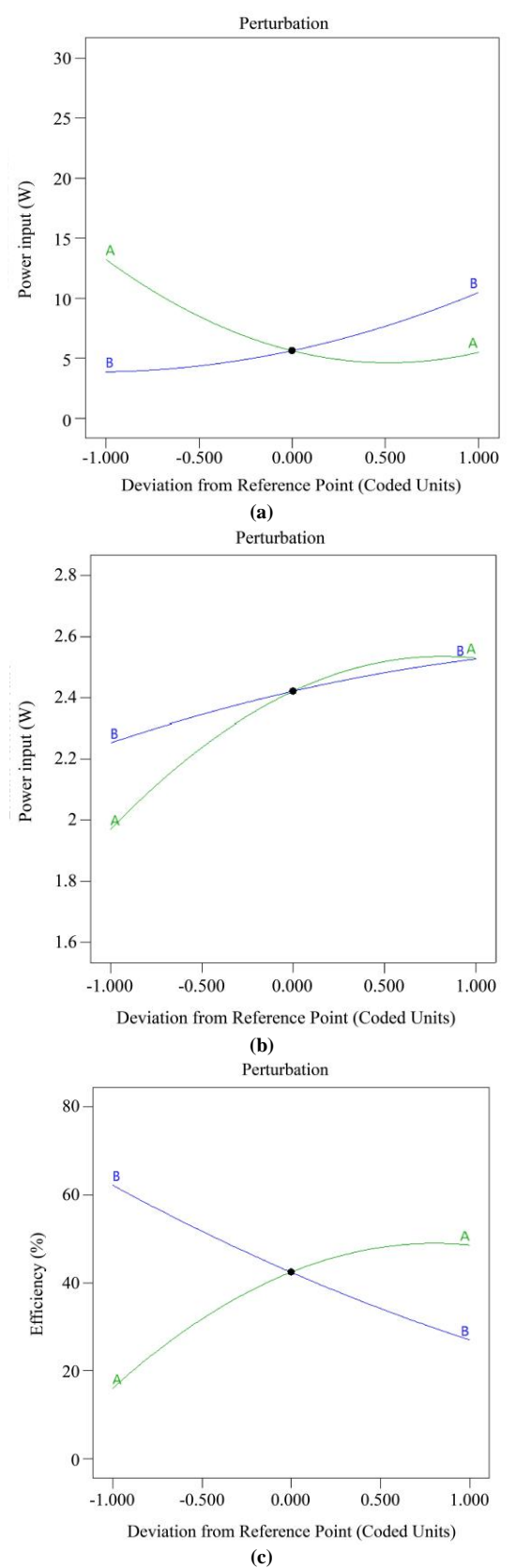


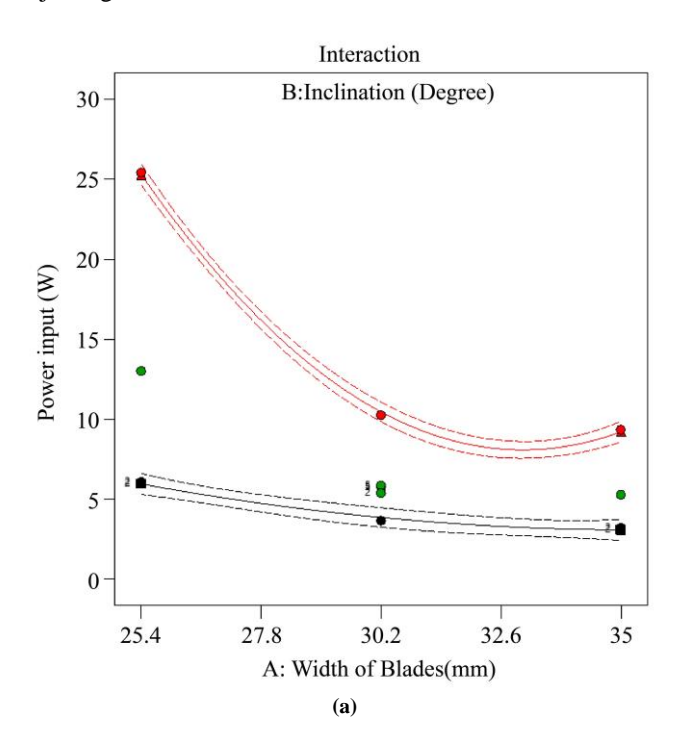
Fig. 8 Perturbation plot, (a) Power input, (b) Power output, and (c) Efficiency.

Interaction plots (Figure 9) help assess whether one factor's effect depends upon another level's. Lines will intersect greatly if they are not parallel. Blade width, along with inclination angle, interacts greatly since the interaction plot (Figure 9(a)) displays lines that are also strongly non-parallel.

This display indicates a very important interaction. It is because the effect of blade width on power input changes based on the inclination angle, and vice versa, that this is what it means. At a low inclination angle, for example, increasing blade width has a minimal effect on power input. However, just that same change in blade width does cause a substantial increase in the power input when the inclination angle is indeed high.

Nearly parallel to each other are lines in the interaction plot for power output (Figure 9(b)). This visual evidence supports the ANOVA result (p = 0.6631 for the AB term), which found no important interaction for this response between inclination angle and blade width. Thus, the two factors do seem to be affecting power output independently, for the most part.

For purposes of efficiency (Figure 9(c)), the lines are obviously not parallel because they do indeed confirm the important interaction effect identified in the ANOVA (p=0.0002). The benefit to efficiency from a wider blade at a shallow angle (20°) is clearer in the plot than at a steep angle (35°). This synergistic effect is vital for optimization work. Efficiency at its highest comes from factor levels in a specific combination, like wide blades at a shallow angle, not from adjusting each factor to its extreme.



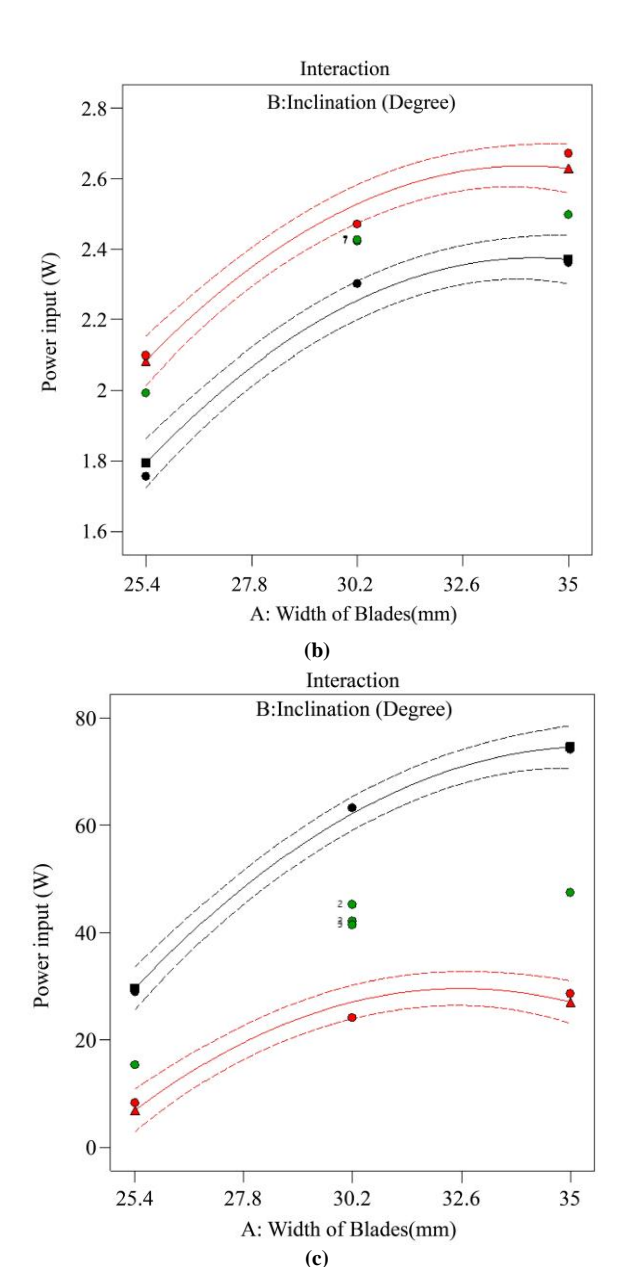


Fig. 9 Interaction plot, (a) Power input, (b) Power output, and (c) Efficiency.

4.4. Optimum Condition for Power Input, Power Output, and Efficiency

Figure 10 presents a desirability function that stems from the process's optimization, so the process considers power input, power output, and efficiency as responses. The model procured a value near unity since the desirability scale existed from 0 to 1. Integrated desirability measurement includes this value. The comparatively elevated result evinces that this particular parameter amalgamation provides a completely adequate conciliation between those disparate goals. It guarantees the turbine functions skillfully while sustaining helpful input and output power values. The smooth proclivity of the desirability function evinces that the optimization protocol efficaciously arrayed the projected responses as it executed and attained its established performance objectives.

The related best design values are shown in Table 8. The assessment was executed close to the superior border of the examined spectrum. Consequently, a prime blade breadth of nearly 35.0 mm came to light. Through engagement with an increased effective water area, wider blades are able to perform much better in the turbine for the purpose of transferring more energy, in addition to generating more torque, which indicates. In contrast, the ascertained supreme cant angle totaled 20.5°. This value was in proximity to the experimental range's boundary. Since a diminished inclination angle curtails turbulence and minimizes hydraulic losses, the blades interact with smoother water flow. Utilizing such prime configurations, power consumption diminished to 3.183 W, and this equaled the minimal tenable figure inside the design area. The turbine furnished scant energy yet yielded a comparatively high power of 2.386 W, nearing the maximum anticipated output of 2.671 W. This evinces that the design configuration can derive large energy from a meager input and stresses that it is apt for low-head, small-scale hydropower applications. It reached 72. An efficiency figure of 85.93% is realized under that optimal circumstance, approximating the 74.16% experimental ceiling. Energy conversion is achieved through selected factor levels. This validates that the designated factor standards possess that skill. Energy that is transformed does show great efficacy.

These indicate overall that the screw turbine performs optimally at an inclination near 20.5° and a blade width near 35.0 mm. The turbine can maximize output power and efficiency while minimizing input power requirements in these conditions. Elevated desirability confirms optimization outcomes are indeed strong. This design could yield efficient, sustainable micro-hydropower generation, as this validation highlights.

Table 8. Optimal values of the designed factors and the response of the screw turbine

_							
Metrics	Target	Minimum	Maximum	Optimal Values			
Width of blades (mm)	In range	25.4	35	35.0			
Inclination Angle (°)	In range	20°	35°	20.50			
Power input (W)	In range	3.18341	25.4081	3.18341			
Power Output (W)	In range	1.7563	2.6715	2.38563			
Efficiency (%)	Maximum	8.25801	74.1595	72. 8593			
Desirability	-	0	1	0.980			

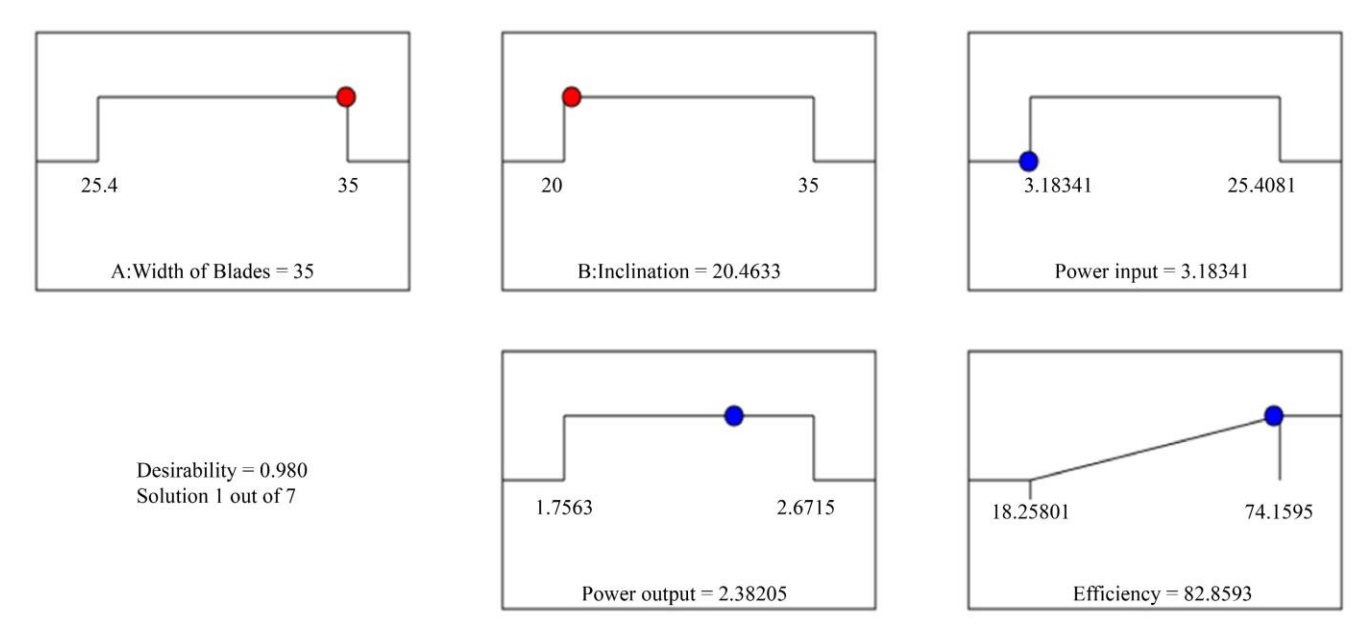


Fig. 10 Desirability for optimization of parameters for power input, power output, and efficiency



Fig. 11 Prototype of portable Archimedean screw turbine

4.5. Comparative Results to Existing Study

The present study of a portable Archimedean screw turbine (Figure 11) shows that turbine inclination, along with blade width, is the most influential parameter because they govern performance. Response Surface Methodology analysis revealed that optimum conditions were able to be attained at an inclination angle of approximately 20.5° and at a blade width of 35 mm. An efficiency of 72. 8593% with minimal power input of 3.18 W was achieved under these conditions. At a 35° inclination, a maximum efficiency of 74.2% was experimentally recorded at that point.

Earlier studies generally agree with these results. Optimum efficiency at relatively shallow inclinations of 20–25° has been reported through several experimental and numerical studies, which aligns with the predicted optimum from the present RSM analysis [15]. Comparable experimental prototypes show reported efficiency levels

ranging typically from 50–80%. This range corresponds well to the present experimental efficiency [15]. In contrast, higher efficiencies, which exceed 85–90%, are often documented within computational or large-scale models. These models minimize both leakage and boundary effects and suggest that localized maxima can occur within narrow design spaces.

Another aspect deviates from what the power outputs absolutely do. Its micro-scale design, along with low discharge (10⁻³–10⁻⁴ m³/s), resulted in a prototype's maximum value of 2.67 W. Outputs ranging from tens up to hundreds of watts are reported for larger-scale devices [4]. Scales with flow conditions mainly account for such differences rather than inefficiency. Efficiency improves because inclination is still the most sensitive parameter, as shallow slopes reduce leakage plus bucket filling. Viscous and incidence losses eventually dominate [8, 24]. These present results reinforce this principle. Ideal angles, though, might change under

limited flow and stress states, considering linked parameter impacts (width × inclination). Blades widen, improving torque capture; dataset quadratic trends confirm eventual performance saturation similar to past CFD simulations [17].

This work's three key contributions benefit from existing literature. Unlike some former studies, they highlight a gradient with passage factors; this analysis carefully assesses vane breadth via a planned RSM tactic. Second, the study provides experimentally validated optima regarding microscale, low-head operation, as it offers actionable design guidance specifically (20.5°; 35.0 mm width) for pico-hydro applications. The analysis clarifies that curvature dominates efficiency optimization instead of strong parameter interaction; thus, design focus should refine future AST development.

Table 9. Comparative overview of Archimedean screw turbine studies

Reference	Turbine Type	Key Parameters Investigated	Achieved Efficiency (%)	Key Findings
[8]	Archimedean Screw Turbine (experimental, multi-blade)	Inclination angle, number of blades	65–79%	I found higher efficiency at 20- 24.5° with five blades; I highlighted tradeoffs between blade number and angle.
[11]	Mini Portable Archimedean Screw Turbine (prototype, low- flow rivers)	Shaft bias angle (45°)	94.6%	Achieved very high efficiency in low-flow rivers in Malaysia, though at a steeper angle than is typically found optimal.
[12]	Archimedean Screw Turbine (numerical & experimental validation)	Inclination angle, flow rate	~70–80%	Validated CFD models against experimental data, confirming optimal performance in the 20-25° inclination range.
[15]	Archimedean Screw Turbine (experimental prototype)	Inclination angle, flow rate	50-80%	Tested different inclination angles (20–25° optimum).
[23]	Archimedean Screw Turbine (run-of-river application)	Inclination angle, scaling effects	~75%	Highlighted the dominant effect of inclination angle on performance in practical run-of-river applications.
[24]	Archimedean Screw Turbine (lab-scale, optimization study)	Inclination angle, flow rate	60–78%	Demonstrated efficiency improvement through systematic parameter tuning, reinforcing the value of optimization studies.
[25]	Portable Archimedean Screw Turbine	Tilt angle (22°), screw length (0.8m)	55.6 (max)	Proved the feasibility of a small, low-cost AST for community-scale generation, albeit with moderate efficiency.
Present Study	Portable Archimedean Screw Turbine (PVC, lightweight)	Blade width (35.0 mm), Inclination angle (20.5°)	72.8593% (optimum), max 74.1595%	Systematically optimized a lightweight, PVC-based design using RSM, providing a validated framework for low-cost, decentralized applications.

4.6. Limitations and Future Research

This study provides a validated framework for optimizing a portable PVC-based AST, suggesting avenues for future research, which is important to acknowledge its limitations.

First, the prototype is a pico-scale model tested under specific field conditions. Larger systems or different hydrological environments may not be directly scalable to the optimal parameters derived here. The principles for the optimization methodology are transferable. However, in the

event that locations feature different head and flow characteristics, site-specific optimization is required to deploy. The optimization's scope was limited to two geometric parameters, specifically the inclination angle and blade width. Screw pitch and blade number largely influence AST performance, for example. Performance is also influenced by the clearance gap between the blades and the trough [11, 15]. RSM could be used at some point in future studies to develop a more thorough multi-parameter optimization model. These are studies that could incorporate additional variables.

Third, discharge measurement relied upon a manual datagathering method. This method, while care had been taken to ensure consistency, is also intrinsically less precise than a calibrated in-stream flowmeter. Improved instruments will help experiments go forward by lessening uncertainty when measuring. Finally, the initial performance optimization is what this study focuses on. Further investigation is required regarding the long-term performance and durability of the PVC construction under environmental exposure, mechanical stress, and continuous operation, as discussed in the following section.

4.7. In-Depth Analysis of PVC Long-Term Performance

A critical consideration for the long-term viability of the proposed generator is just how durable PVC remains in an outdoor aquatic environment when subjected to continuous mechanical stress. PVC has superb durability and intrinsic waterproofness, coupled with high resistance to chemical and biological corrosion. For applications such as underground piping, there is an estimated service life exceeding 50-100 years [26]. These properties make hydropower a fundamentally suitable material for hydropower applications. One must consider that two primary mechanisms degrade a turbine application, however: Ultraviolet (UV) radiation exposure and effects from combined mechanical stress when water immerses.

- Sunlight causes unprotected PVC undergo photodegradation from UV degradation. This process is largely superficial, and discoloration, a brownish tint, occurs. The outer layer that is exposed also sees a reduction in impact strength [27]. Crucially, studies have shown that this degradation penetrates the material less than 0.05 mm (0.002 inches) along with having no practical effect on the pipe's tensile strength or modulus of elasticity, which handle pressure and structural loads as key properties [28]. UV inhibitors such as rutile titanium dioxide (TiO2) can be incorporated into the PVC formulation throughout manufacturing for the purpose of effectively reducing this superficial embrittlement, or a coat that is simply containing light-colored, water-based latex paint can be applied to the exposed surfaces [28].
- 2. Hydro-mechanical Stress: The turbine blades will be subject to continuous hydrodynamic loading. This is on account of the blades being underwater. Extended submersion in water in combination with stress can slowly remove plasticizers and other additives from PVC [29]. Material brittleness may increase over time because of this process, increasing fatigue cracking or failure risk

[29]. PVC absorbs little water (typically 0.04-0.4% over 24 hours), yet a turbine blade's dynamic loading cycle is more demanding than static applications like piping.

Therefore, the fundamental properties of PVC are very favorable. Characterizing its full performance lifecycle as a turbine material requires long-term field deployment and periodic material testing. Future research should focus on long-term monitoring of blade integrity, investigate potential creep and fatigue, and explore using UV-stabilized PVC grades to improve operational longevity.

5. Conclusion

This study demonstrated the successful development into optimization of a lightweight, portable hydro generator because it employed an Archimedean screw, PVC, and screen filtration, and addressed the challenge of sustainable energy provision for low-head water applications.

The application of response surface methodology and variance analysis confirmed that the blade width and inclination angle primarily determine system performance, as these factors affect power input, power output, and efficiency through both linear and quadratic interaction effects. Optimization revealed that a blade width of 35.0 mm and an inclination angle of 20.5° yielded an efficiency of 72.8593% at minimal input power (3.18 W) with near-maximum output, underscoring the robustness of the proposed design. Since the high coefficient of determination "R2" values together with predictive validity as well as model adequacy verified through non-significant lack-of-fit tests, assurance in the derived optima is ensured.

These discoveries substantiate previous research by furnishing empirically confirmed parameter boundaries. They additionally augment previous scholarship concerning microscale Archimedean screw turbines. In lieu of factors plainly interplaying, optimizing efficiency accentuates the curve's non-linear function. The analysis, hypothetically, may assist individuals in comprehending spatial and functional variables within compact hydroelectric configurations, and realistically, it may permit individuals to construct a budget-friendly architecture for distributed power generation via regionally accessible resources. Researchers should probe modular configurations with alternative lightweight composites. Furthermore, they should explore methods for improved waste administration. Its applicability will expand over time because it scales more effectively and functions more strongly off-grid.

References

- [1] Hanane Allioui, and Youssef Mourdi, "Exploring the Full Potentials of IoT for Better Financial Growth and Stability: A Comprehensive Survey," *Sensors*, vol. 23, no. 19, pp. 1-68, 2023. [CrossRef] [Google Scholar] [Publisher Link]
- [2] Benjamin K. Sovacool et al., "Equity, Technological Innovation and Sustainable Behaviour in a Low-Carbon Future," *Nature Human Behaviour*, vol. 6, pp. 326-337, 2022. [CrossRef] [Google Scholar] [Publisher Link]

- [3] Meita Rumbayan, and Rilya Rumbayan, "Feasibility Study of a Micro Hydro Power Plant for Rural Electrification in Lalumpe Village, North Sulawesi, Indonesia," *Sustainability*, vol. 15, no. 19, pp. 1-13, 2023. [CrossRef] [Google Scholar] [Publisher Link]
- [4] Nouman Khan et al., "Development of a Sustainable Portable Archimedes Screw Turbine for Hydropower Generation," *Scientific Reports*, vol. 15, pp. 1-17, 2025. [CrossRef] [Google Scholar] [Publisher Link]
- [5] Arash YoosefDoost, and William David Lubitz, "Archimedes Screw Turbines: A Sustainable Development Solution for Green and Renewable Energy Generation—A Review of Potential and Design Procedures," *Sustainability*, vol. 12, no. 18, pp. 1-34, 2020. [CrossRef] [Google Scholar] [Publisher Link]
- [6] Wim Jonker Klunne, "Barriers to the Uptake of Small Hydropower for Rural Electrification in Africa," *Proceedings of the 30th ISES Biennial Solar World Congress 2011*, Kassel, Germany, pp. 1-9, 2011. [CrossRef] [Google Scholar] [Publisher Link]
- [7] A.A. Lahimer et al., "Research and Development Aspects of Pico-Hydro Power," *Renewable and Sustainable Energy Reviews*, vol. 16, no. 8, pp. 5861-5878, 2012. [CrossRef] [Google Scholar] [Publisher Link]
- [8] Guilhem Dellinger et al., "Effect of Slope and Number of Blades on Archimedes Screw Generator Power Output," *Renewable Energy*, vol. 136, pp. 896-908, 2019. [CrossRef] [Google Scholar] [Publisher Link]
- [9] Dianne Mae M. Asiñero, Antonio-Abdu Sami M. Magomnang, and Joel L. Asiñero, "Design and Performance Evaluation of a Double-Bladed Archimedean Screw Turbine for Low-Head Hydropower Generation," *Journal of Biodiversity and Environmental Sciences*, vol. 25, no. 4, pp. 1-11, 2024. [Publisher Link]
- [10] Emmanuel Ighodalo Okhueleigbe, and Ofualagba Godswill, "Mini-Hydro Turbine: Solution to Power Challenges in an Emerging Society with Abundance of Water," *American Journal of Engineering and Technology Management*, vol. 2, no. 2, pp. 7-12, 2017. [CrossRef] [Google Scholar] [Publisher Link]
- [11] Man Djun Lee, and Pui San Lee, "Modelling the Energy Extraction from Low-Velocity Stream Water by Small Scale Archimedes Screw Turbine," *Journal of King Saud University Engineering Sciences*, vol. 35, no. 5, pp. 319-326, 2023. [CrossRef] [Google Scholar] [Publisher Link]
- [12] Zeshan Abbas et al., "Numerical and Experimental Investigation of an Archimedes Screw Turbine for Open Channel Water Flow Application," *Energy Science & Engineering*, vol. 12, no. 4, pp. 1317-1336, 2024. [CrossRef] [Google Scholar] [Publisher Link]
- [13] Maël Bouvant et al., "Design Optimization of an Archimedes Screw Turbine for Hydrokinetic Applications using the Response Surface Methodology," *Renewable Energy*, vol. 172, pp. 941-954, 2021. [CrossRef] [Google Scholar] [Publisher Link]
- [14] W.O. Adedeji et al., "Utilization of the Pico-Scale Turgo Turbine for Rural Electrification: A Review," *UI Journal of Civil Engineering and Technology*, vol. 6, no. 2, pp. 1-11, 2024. [Google Scholar]
- [15] Erinofiardi Erinofiardi et al., "Sustainable Power Generation Using Archimedean Screw Turbine: Influence of Blade Number on Flow and Performance," *Sustainability*, vol. 14, no. 23, pp. 1-25, 2022. [CrossRef] [Google Scholar] [Publisher Link]
- [16] Emanuele Quaranta, and Peter Davies, "Emerging and Innovative Materials for Hydropower Engineering Applications: Turbines, Bearings, Sealing, Dams and Waterways, and Ocean Power," *Engineering*, vol. 8, pp. 148-158, 2022. [CrossRef] [Google Scholar] [Publisher Link]
- [17] Isidro Antonio V. Marfori, Alvin B. Culaba, and Aristotle T. Ubando, "Empowering Rural Electrification in the Philippines: A Case Study," *Journal of the British Academy*, vol. 11, no. s7, pp. 33-51, 2024. [CrossRef] [Google Scholar] [Publisher Link]
- [18] Clare Richardson-Barlow et al., Facilitating a Just, Fair, and Affordable Energy Transition in the Asia-Pacific, The British Academy, pp. 1-31, 2022. [Google Scholar] [Publisher Link]
- [19] Sari Murni et al., "The Role of Micro Hydro Power Systems in Remote Rural Electrification: A Case Study in the Bawan Valley, Borneo," *Procedia Engineering*, vol. 49, pp. 189-196, 2012. [CrossRef] [Google Scholar] [Publisher Link]
- [20] Dowon Han et al., "Design, Fabrication, and Performance Test of a 100-W Helical-Blade Vertical-Axis Wind Turbine at Low Tip-Speed Ratio," *Energies*, vol. 11, no. 6, pp. 1-17, 2018. [CrossRef] [Google Scholar] [Publisher Link]
- [21] Arash Moradzadeh et al., "Optimal Sizing and Operation of a Hybrid Energy Systems via Response Surface Methodology (RSM)," *Scientific Reports*, vol. 14, pp. 1-14, 2024. [CrossRef] [Google Scholar] [Publisher Link]
- [22] Vipin Uniyal, Ashish Karn, and Varun Pratap Singh, "Parametric Optimization of Archimedes Screw Turbine by Response Surface Methodology and Artificial Neural Networks," *Journal of Renewable Energy and Sustainable Development (RESD)*, vol. 10, no. 2, pp. 306-318, 2024. [CrossRef] [Google Scholar] [Publisher Link]
- [23] Scott Simmons, Guilhem Dellinger, and William David Lubitz, "Effects of Parameter Scaling on Archimedes Screw Generator Performance," *Energies*, vol. 16, no. 21, pp. 1-22, 2023. [CrossRef] [Google Scholar] [Publisher Link]
- [24] Neeraj Kumar Thakur et al., "Efficiency Enhancement in Archimedes Screw Turbine by Varying Different Input Parameters An Experimental Study," *Materials Today: Proceedings*, vol. 52, pp. 1161-1167, 2022. [CrossRef] [Google Scholar] [Publisher Link
- [25] RD. Kusumanto, M. Noviansyah Nugraha, and Indrayani, "Archimedes Screw Turbine Application on Portable Mini Hydropower Plant," *Polymachine Journal*, vol. 21, no. 1, pp. 88-92, 2023. [Google Scholar] [Publisher Link]
- [26] Steven Folkman, "Validation of the Long Life of PVC Pipes," *Proceedings of the 17th Plastic Pipes Conference (PPXVII)*, Chicago, Illinois, USA, pp. 1-9, 2014. [Google Scholar] [Publisher Link]

- [27] K.G. Alahapperuma, and A.M.P.B. Samarasekara, "Degradation of Unplasticised Poly Vinyl Chloride based Engineering Products upon Exposure to Ultra Violet Radiation," *Tropical Agricultural Research*, vol. 30, no. 4, pp. 117-123, 2019. [CrossRef] [Google Scholar] [Publisher Link]
- [28] John Houle, "UV Exposure/Sun Fading Has No Practical Effects On PVC Pipe Performance," PVC Pipe Association, 2024. [Publisher Link]
- [29] Houcine Jemii et al., "Mechanical, Thermal and Physico-Chemical Behavior of Virgin and Hydrothermally Aged Polymeric Pipes," *Journal of Thermoplastic Composite Materials*, vol. 35, no. 12, pp. 2310-2330, 2020. [CrossRef] [Google Scholar] [Publisher Link]